Desalination and Water Treatment
www.deswater.com

doi:10.5004/dwt.2019.24193

160 (2019) 276–287
August

Sorption profile of mercury (II) from aqueous solution onto low-rank Pakistani coal

Tariq Javed[a,c,*], Nasir Khalid[b,*], Nasira Sareecha[a], Muhammad Latif Mirza[a]

[a]*Department of Chemistry, The Islamia University of Bahawalpur, Bahawalpur, Pakistan, Tel. 923455652137, email: jtariq56@yahoo.com (T. Javed), Tel. 923017185509, email: nsareecha@hotmail.com (N. Sareechsa), Tel. 923026825055, email: mlatifmirza@yahoo.com (M.L. Mirza)*
[b]*Chemistry Division, Pakistan Institute of Nuclear Science and Technology, P.O. Nilore, Islamabad, Pakistan, Tel. 923335154870, Fax 925449270462, email: nasirk1953@gmail.com (N. Khalid)*
[c]*Department of Chemistry, University of Sahiwal, Sahiwal, Pakistan*

Received 10 January 2019; Accepted 30 March 2019

ABSTRACT

The adsorption of mercury ions on low-rank Pakistani coal (LPC) has been studied as a function of shaking time, nature of electrolytes ($HClO_4$, H_2SO_4 and HNO_3), dose of adsorbent, metal ion concentration and temperature. The radio tracer technique was applied to examine the distribution of mercury (Hg^{2+}) using a batch method. Maximum adsorption was found to be at 0.0001 mol L^{-1} of HNO_3 solution, using 0.15 g of adsorbent for 4 mL of 4.985×10^{-4} mol L^{-1} mercury concentration with equilibration time of 10 min. The adsorption of mercury was decreased with the increase in the concentrations of all the mineral acids used. The kinetic data indicated an intra particle diffusion process with sorption being pseudo-second order. The determined rate constant k_2 was 0.449 g mg^{-1} min^{-1}. The adsorption data obeyed the Langmuir, Freundlich and Dubinin-Radushkevich isotherm plots over the mercury concentration range of 4.985×10^{-4} to 2.991×10^{-3} mol L^{-1}. The characteristic Freundlich constants i.e. $1/n = 0.160$ and $K = 1.052 \times 10^{-1}$ m mol g^{-1} whereas the Langmuir constants $Q = 3.531 \times 10^{-2}$ m mol g^{-1} and $b = 28.522 \times 10^3$ dm^3 mol^{-1} have been calculated for the adsorption system. The uptake of mercury was increased with the rise in temperature (283–333 K). Thermodynamic quantities i.e. ΔH, ΔG and ΔS have been computed and discussed for the system. Sorbent was characterized by using SEM and FT-IR before and after the adsorption of mercury. Effect of diverse ions on the adsorption of mercury has also been investigated. Removal of mercury from tap water sample shows the applicability of the proposed method.

Keywords: Low-rank Pakistani coal; Mercury removal; Kinetic; Thermodynamic; Diverse ions

1. Introduction

The presence of heavy metals in waste waters have led to water toxicity and represents an increasing threat for the human beings, living organisms and the environment [1,2]. In addition to rock leaching due to external effects, the contaminated water is generated from different anthropogenic sources such as chemical production, power plants, pharmaceutical manufacturing, mining, painting, electroplating and metallurgy [3–6]. Mercury is a non biodegradable and has been listed by the United States Environmental Protection Agency (USEPA) as a priority pollutant as it can easily pass the blood-brain barrier and effect on the brain. According to WHO permissible limit of mercury ions in drinking water is 0.001 mg L^{-1}. When mercury enters aqueous environment, some biological processes change it to methyl mercury, which is highly poisonous and accumulates in fish, in living organisms that eat fish, and in predators that eat fish-eating living organisms [7]. Depending on the concentration of exposure, the effects of mercury exposure can include alteration of the fertility system, minamata disease,

*Corresponding author.

1944-3994 / 1944-3986 © 2019 Desalination Publications. All rights reserved.

slower growth, numbness of the limbs and lips, visual constriction, nervous system disorder and loss of speech, hearing and memory [8,9]. Thus, the removal of this poisonous heavy metal from contaminated water is a critical issue from the health point of view.

A variety of techniques for the removal of mercury ions from effluents have been reported such as coagulation [10,11], cementation [12], solvent extraction [13,14], ultra filtration [15,16], ion exchange [17,18], membrane separation [19,20], chemical precipitation [21,22] and adsorption.

Among these treatment processes, the mercury adsorption method at the solid-liquid interface is a promising and dominant method with some advantages of high efficiency, simplicity, low cost and the availability of diverse adsorbents [23,24] such as activated carbon [25], silicates of aluminum and titanium [26,27], oxides of silicon and aluminum α-Al_2O_3 [28,29], mesoporous SBA-15 [30], carbon aerogel [31], fly ash [32], activated carbon [33], clay [34] and various other adsorbents.

Beside the above mentioned adsorbents the inexpensive coal is also being used for adsorption of heavy metal ions from aqueous solutions. The selected material is abundantly available as a low cost material even after its wide consumption as a fuel in power generation plants, brick kilns and various other mills. The LPC possesses a granular structure, high surface area, highly oxygenated with many carboxyl and phenolic hydroxyl functional groups which are capable to adsorb the metal ions via ion exchange process. Due to the presence of such properties the LPC seems to be a good candidate for adsorbent of mercury ions.

The aim of the present study is to develop a rapid, efficient and cost effective procedure for the removal of mercury ions using abundantly available cheaper LPC as an adsorbent employing radio tracer technique. The low-cost Pakistani coal has also been studied as an adsorbent for the removal of strontium [35], chromium [36], copper [37] and lead [38] from aqueous media. In addition, no work has been reported so far concerning the adsorptive removal of mercury ions using low-rank Pakistani coal.

2. Materials and methods

2.1. Preparation of radio tracer

The radio tracer of mercury ^{203}Hg ($t_{1/2}$ = 47 d) used in this research was prepared by using the nuclear reactor at PINSTECH. A known weight of spec-pure $Hg(NO_3)_2$. H_2O from Johnson & Matthey(UK), was packed in polyethylene capsule, heat sealed and sent for irradiation in Pakistan Research Reactor-I (PARR-I), at a neutron flux of 4.5×10^{13} cm^{-2} s^{-1}. After proper cooling time, the irradiated mercury salt was transferred into a pre-cleaned beaker, dissolved in minimum amount of nitric acid and diluted to a known volume with distilled and deionized water.

2.2. Reagents

LPC was collected from mines in the province of Punjab (Khoshab, Makerwal). The sample was ground and sieved to a particle size of 500 µm. The powdered coal was activated at 300°C in a muffle furnace for 4 h to enhance the basicity of adsorbent. Thermally activated sample was treated with 2 M H_2SO_4 at room temperature for 2 h. The acidic treatment may oxidize the porous coal surface, remove the mineral constituents and improve the hydrophilicity of surface. After H_2SO_4 treatment, the coal was washed with deionized water until the neutral pH of the filtrate. The washed sample was dried at 60°C till constant weight and stored in an air tight plastic container. The LPC sample was characterized by different techniques and standard procedures. All the chemicals used were of Analytical Grade and were used as received.

2.3. Instrumentation

The surface area of low-rank Pakistani coal sample was measured according to Brunauer–Emmett–Teller (BET) method by nitrogen adsorption at 77 K using BET surface area analyzer, Quantachrome AS1-C-8, USA. Before nitrogen adsorption, the sample was degassed for 2 h at final pressure of 133.32×10^{-4} Pa. IR spectra were recorded on a FT-IR spectrophotometer (Tensor 27, Bruker, Germany) in the frequency range of 4000–400 cm^{-1}. The Scanning Electron Microscopy (SEM) images of low-rank Pakistani coal samples (coal and mercury loaded coal) were recorded at different magnifications from 250 to 40,000, using Scanning Electron Microscope (SEM), Joel, Japan.

2.4. Adsorption measurements

A known amount of LPC was added in a 4 ml of standard acid solution or buffer solution of selected pH, along with an appropriate volume of stock radio tracer solution in 25 mL culture tube with a screwed polyethylene cap. The contents were equilibrated on a mechanical shaker for 10 min. and centrifuged for 2 min at a revolution of 5000/min. The supernatant solution was separated. The radioactivities of the liquid phase were determined before and after equilibration with a NaI well type scintillation counter (Canberra Inc.) coupled with a counter scalar (Nuclear Chicago). The percentage adsorption of mercury ions from the solution was calculated using the following expression:

$$\%\ \text{age adsorption} = \frac{A_i - A_f}{A_i} \times 100 \quad (1)$$

where A_i is the initial radioactivity of mercury ions in the solution and A_f is the radioactivity of mercury ions in solution after equilibrium.

The reported values of mercury ions adsorbed are the average of at least three independent measurements. All the measurements were performed at room temperature (297 ± 1 K) unless otherwise specified.

3. Results and discussion

3.1. Characterization of adsorbent:

The low rank Pakistani coal used for the adsorption of mercury was characterized for its various physicochemical

properties such as ash contents, bulk density, BET surface area, total pore volume, average pore diameter, porosity and pH_{pzc} by using instrumental techniques and standard procedures and the determined values were found to be 18.39%, 2.0 g mL^{-1}, 4.8 m^2 g^{-1}, 4.8 × 10^{-3} cc g^{-1}, 4.0 nm, 53 % and 3.1, respectively.

3.1.1. FT-IR studies

The adsorption of mercury ions (Hg^{2+}) on low rank Pakistani coal was verified by observing the perturbation in the absorption peaks in the FT-IR spectra of the samples of coal and mercury loaded coal. The absorption peaks at 2914 cm^{-1} is assigned to for surface O–H stretching. The peaks at 1750, 1429, 1367, 1027, 597 and 581 cm^{-1} are associated with the stretching of C=O, O–H bending, stretching of C–H, stretching of S=O, O–H stretching of –C–O–H group, asymmetric bending of sulphate group and symmetric bending of sulphate group, respectively [39–42].

Following the adsorption of mercury, the IR spectrum of coal exhibited changes in the peak positions. The shifting of absorption peaks at 1750,1367, 597 and 581 cm^{-1} to 1733, 1365, 610 and 583 cm^{-1}, respectively and the disappearance of absorption peak at 1429 cm^{-1} in the spectrum of mercury loaded coal indicates the involvement of carboxylic and sulfonic acid groups during the adsorption of mercury ions on low rank Pakistani coal. Similar observations of minor shifts and decrease in the intensities of the FTIR peaks after the adsorption of metal ions on different biosorbents have been reported [43–45].

3.1.2. SEM and EDX analysis

The morphology of the activated coal was evaluated using scanning electron microscopic (SEM) technique at different magnifications from 250 to 40,000, and those at 20,000 have been shown in Fig. 1. It is clear from Fig. 1A that initially the surface of coal was rough and irregular with many loops and humps. The determined pore size present on the surface of coal was in the range of 160–701 nm, indicating the macro-porous structure of adsorbent [46].

Fig. 1B illustrates the SEM image of coal after adsorption of mercury, with changed surface morphology of the adsorbent i.e., decrease in surface heterogeneity resulting in the smoother surface. The ionic diameter of mercury ions is 0.22 nm, which is much smaller than the pore size present in coal (160–701 nm), enabling adsorption of mercury ions through pore diffusion mechanism. The EDX graph (Fig. 2) shows the presence of six energy peaks of mercury in the range of 1.50 to 10.00 keV. Thus revealing the presence of mercury ions on coal surface as a result of adsorption.

3.2. Influence of electrolytes

The chemical contact plays a significant role in the adsorption process by affecting the surface charge of sorbent, the extent of ionization and speciation of the sorbate. Therefore, the adsorption characteristics of mercury (4.985 × 10^{-4} mol L^{-1}) was investigated in mineral acid solutions (HNO_3, H_2SO_4, $HClO_4$) by varying a concentration range from 0.0001 to 1.0 mol L^{-1} using 4.985 × 10^{-4} mol L^{-1} of mercury with 0.15 g of activated LPC. The concentration of mercury and dose of 0.15 g of coal was selected arbitrarily and the results are presented in Fig. 3. The HCl was not included in this study since it may form insoluble salts with mercury.

Maximum removal of mercury ions was occurred at 1.0 × 10^{-4} mol L^{-1} of acid concentration. With the increase in mineral acid concentration the adsorption of mercury was started decreasing up to 1.0 mol L^{-1}. All the acids studied

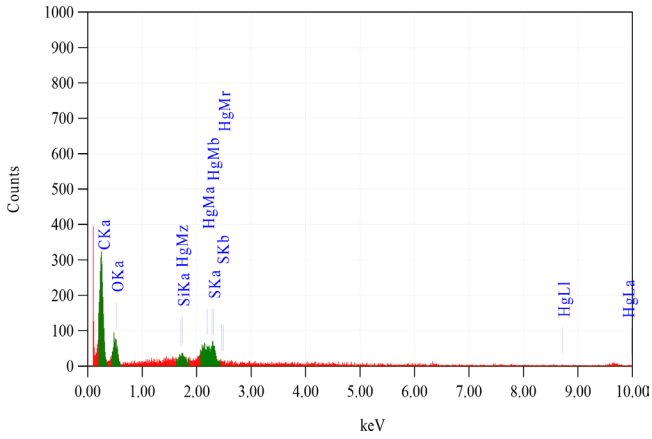

Fig. 2. EDX graph of Hg (II) loaded coal.

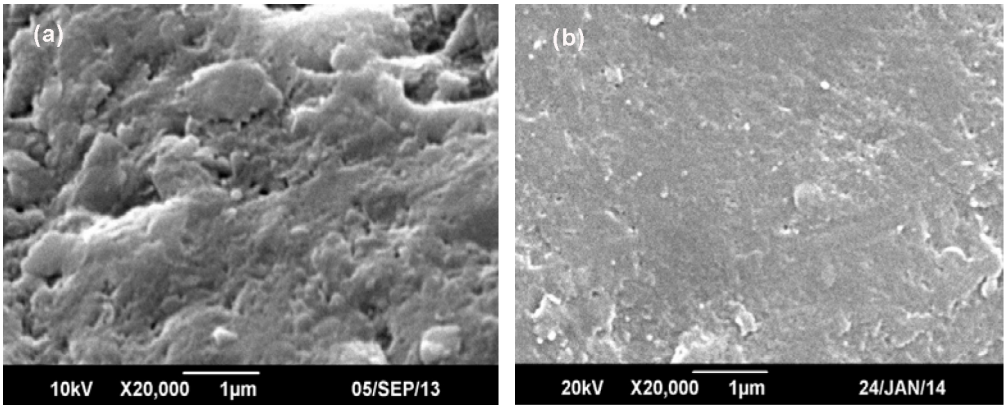

Fig. 1. SEM images of the LPC before (A) and after (B) mercury adsorption.

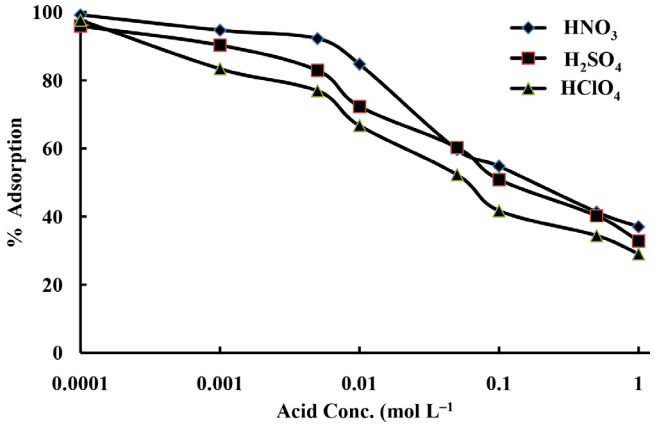

Fig. 3. Variation of adsorption of mercury ions on LPC as a function of acid concentration.

show same sorption pattern. At higher acid concentration, the surface ligands were closely associated with the hydrogen ions as compare to positively charged mercury ions. As the concentration of acid decreased, more ligands such as carboxyl, sulfonyl would be exposed and carried negative charges with subsequent attraction of positively charged mercury ions and higher adsorption onto surface of LPC.

Maximum removal of mercury ions at 1.0×10^{-4} mol L^{-1} of acid concentration on LPC is in accordance with the concept of zero-point charge, which is 3.1. Above point of zero charge the coal surface possess negative charge which facilitates in the enhanced electrostatic attractions between positively charged mercury ions and negatively charged LPC surface. A pH value of 4.0 has been reported for the maximum adsorption of cadmium and mercury on low rank Turkish coal [47,48] and cadmium and lead on leonardite [49].

The adsorption of mercury ions on LPC surface could be explained via ion exchange mechanism according to the following relations.

$$m[Coal-OH] \rightleftharpoons m[Coal-O]^{-} + mH^{+} \quad (2)$$

$$M^{n+} + m[Coal-O]^{-} \rightleftharpoons M[Coal-]_{m}^{(n-m)} \quad (3)$$

The overall reaction could be represented as:

$$m[Coal-OH] + M^{n+} \rightleftharpoons M[Coal-]_{m}^{(n-m)} + mH^{+} \quad (4)$$

where [Coal–OH] = activated coal surface; M^{n+} = metal ions with n + charge; mH^{+} = number of protons released.

The Eq. (2) represents deprotonation of the activated coal while Eq. (3) shows the attachment of the metal ions on the coal surface. At lower pH values the H^{+} ions compete for binding sites on the coal surface, resulting a limited interaction of Hg(II) ions with the binding sites because of higher repulsive force that arises.

It was also observed that maximum adsorption of mercury ions occurred at 0.0001 mol L^{-1} HNO_3 as compared to the other mineral acids; therefore, this concentration of HNO_3 was selected for all the subsequent experiments regarding the optimization of adsorption parameters for mercury ions on LPC.

3.3. Effect of LPC dose

Effect of the LPC dose on Hg(II) adsorption was studied by varying the LPC dose from 0.025 to 0.5 g using 4.0 mL of 4.985×10^{-4} mol L^{-1} of mercury solution at 0.0001 mol L^{-1} of HNO_3 for time interval of 10 min. It is clear from Fig. 4, which is a plot of percentage adsorption of mercury vs. LPC dose, that percentage adsorption increases with an increase in the adsorbent dose. This is because by increasing the LPC dose, the number of active sites available for LPC-mercury interaction is increased as well. Just 0.15 g of adsorbent is sufficient for the quantitative adsorption of mercury solution used beyond which percentage adsorption was almost constant. Therefore, LPC dose of 0.15 g was considered to be sufficient for the adsorption of mercury and was selected for all further investigations.

3.4. Effect of shaking time

The effect of shaking time on the removal of Hg(II) was studied by varying the time from 0.5 to 15 min using 4.0 mL of 4.985×10^{-4} mol L^{-1} mercury solution in 0.0001 mol L^{-1} of HNO_3 using 0.15 g of LPC and the results are shown in Fig. 5.

The observed increase in percentage adsorption with increase in contact time could probably be due to more time require for Hg(II) ions to interact with LPC up to 10 min after this no considerable increment was observed because of unavailability of active sites. Therefore, 10 min shaking time was considered for further investigations.

The mercury can be removed from the liquid medium to the surface binding sites of the LPC through different processes. The process may involve film or pore diffusion, external diffusion, surface diffusion and adsorption on the pore surface. The overall sorption may involve one or more steps. The sorption data was applied to the Morris-Weber expression [50]:

$$Q_t = K_{\text{int}} t^{0.5} \quad (5)$$

where Q_t (mg g^{-1}) is the sorbed concentration of mercury at time (t). K_{int} is the intra particle diffusion rate constant of the Morris-Weber equation.

The value of K_{int} was determined from the slope by plotting q_t against $t^{0.5}$ (Fig. 6) and was found to be 4.13×10^{-1} mg/ (g $\text{min}^{0.5}$). Fig. 6 depicts that the adsorption of mercury ions was rapid up to 6 min and then slowed down up to 15 min, which is clear from two distinct slopes of 0.730 and 0.105 for the first 0.5–6 min and 7–15 min respectively [51].

The nature of the adsorption either via film diffusion or intra particle diffusion mechanism was verified by using the Reichenberg [52] equation:

$$X = \left(1 - \frac{6}{\pi^2}\right) e^{-\beta_t} \quad (6)$$

where $X = \dfrac{Q_t}{Q_e} = \dfrac{Amount\ of\ metal\ adsorbed\ at\ time\ "t"}{Amount\ of\ metal\ adsorbed\ at\ equilibrium}$

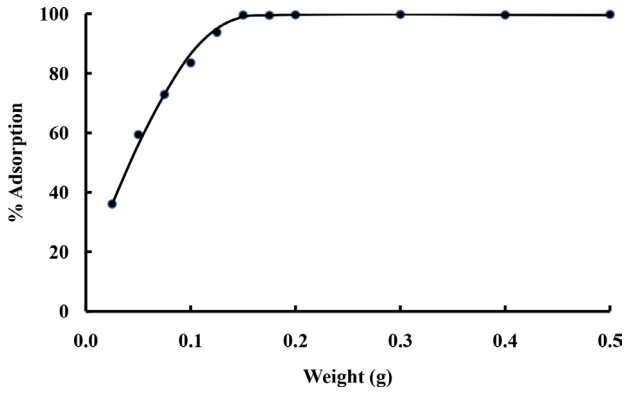

Fig. 4. Effect of LPC dose on the adsorption of mercury.

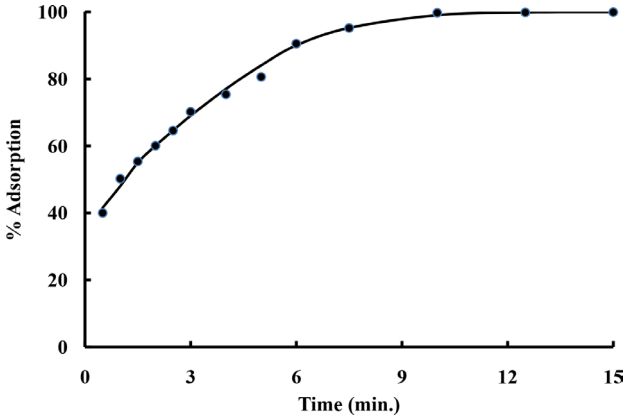

Fig. 5. Effect of shaking time on the adsorption of mercury on LPC.

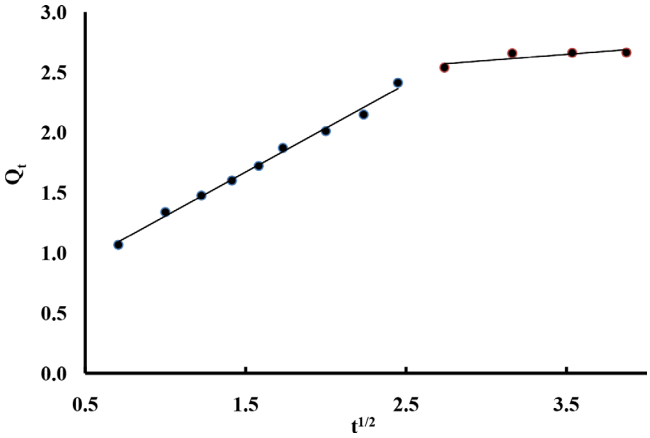

Fig. 6. Morris-Weber plot of mercury ions adsorption on LPC.

The value of β_t is a mathematical function of X that can be calculated for each value of X by using the equation:

$$\beta_t = -0.4977\ \ln(1-X) \tag{7}$$

The plot of β_t vs. time is a straight line (Fig. 7) with a correlation factor of 0.9953 which indicates that the sorption is controlled by film diffusion.

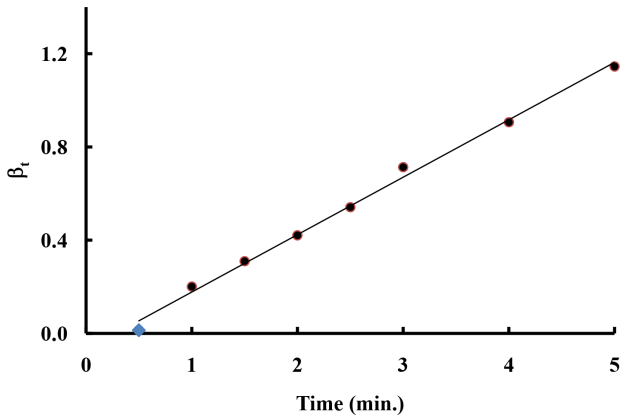

Fig. 7. Reichenberg plot of mercury adsorption on LPC.

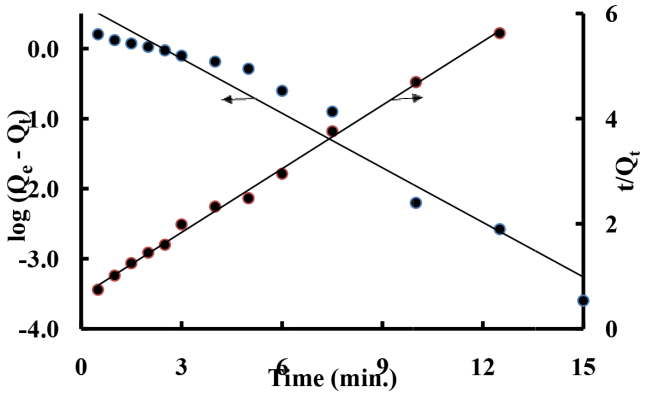

Fig. 8. Pseudo first order and pseudo second order plots of mercury ions adsorption on LPC.

In order to evaluate kinetic adsorption parameters the obtained time dependent adsorption data of mercury ions on LPC was subjected to the first order Lagergren [Eq. (8)] and pseudo-second order [Eq. (9)] rate expressions using the linearized form as:

$$\log(q_e - q_t) = \log q_e - \frac{k_1}{2.303}t \tag{8}$$

$$\frac{t}{q_t} = \frac{1}{k_2 q_e^2} + \frac{1}{q_e}t \tag{9}$$

where q_e is the amount of mercury adsorbed at equilibrium (mg g^{-1}), q_t is the amount of mercury adsorbed at any time t (mg g^{-1}), t is the time (min) and k_1 (min^{-1}) and k_2 (g mg^{-1} min^{-1}) are the rate constants of the pseudo-first order and second order relationships, respectively. The linear plots were obtained by plotting log ($q_e - q_t$) against t and t/qt vs. t with correlation coefficients (R^2) of 0.990 and 0.992 for the pseudo-first order and second order models, respectively. The results are depicted in Fig. 8 and the determined kinetic parameters for the pseudo-first order and second order models have been summarized in Table 1.

The pseudo second order model is commonly used to predict the adsorption process over the whole range of adsorption. The higher R^2 value and good correspondence

Table 1
Kinetic data for the adsorption of mercury ions on LPC

Pseudo first order			Pseudo second order		
q_e (mg g^{-1})	k_1 (min^{-1})	R^2	q_e (mg g^{-1})	k_2 (g mg^{-1} min^{-1})	R^2
1.736	0.246	0.995	2.463	0.449	0.989

Experimentally calculated q_e = 2.665 mg g^{-1}

with the calculated (2.463 mg Hg g^{-1}) and experimental (2.665 mg Hg g^{-1}) values of adsorption capacity confirm that the experimental kinetic data is more favorable with the pseudo-second order rate expression.

3.5. Effect of initial mercury ion concentration

The effect of mercury concentration on the efficiency of adsorption was investigated under the optimized conditions of contact time 10 min., adsorbent dose 0.15 g and 0.0001 mol L^{-1} of HNO_3. The initial concentration of mercury was varied from 4.985 × 10^{-4} to 2.991 × 10^{-3} mol L^{-1} and the results are shown in Fig. 9. The percentage adsorption decreased with an increase in the concentration of mercury. This is due to the relatively less number of active sites in a fixed amount of LPC at higher concentration of mercury.

3.5.1. Adsorption isotherms

It is important to study the most appropriate process for equilibrium plots, to optimize the design of an adsorption method. Fruendlich, Langmuir and Dubinin-Radushkevich (D-R) isotherm models were applied to describe the adsorption equilibrium. Experimental isotherm data were carried under optimized parameters for different concentrations of mercury.

3.5.1.1. Fruendlich isotherm

Fruendlich isotherm is the relationship between the concentration of concern metal uptake per unit mass of the adsorbent (C_{ad}) and the concentration of metal at equilibrium (C_e), which is mathematically shown as:

$$C_{ad} = KC_e^{\frac{1}{n}} \tag{10}$$

The Logrithmic form of the above expression (10) can be written as:

$$\log C_{ad} = \log K + \frac{1}{n}\log C_e \tag{11}$$

where *1/n* and *K* are Fruendlich constants indicating the intensity of adsorption and adsorbent capacity respectively. These constants were determined from the slope and intercept of the Fruendlich isotherm (Fig. 10) and were found to be 0.160 and 1.052 × 10^{-1} m mol g^{-1} respectively. The fractional value of the adsorption affinity ($1/n$) is < 1, which corresponds to a hetrogenous surface of the LPC [53]. The determined adsorption capacity of mercury ions on LPC

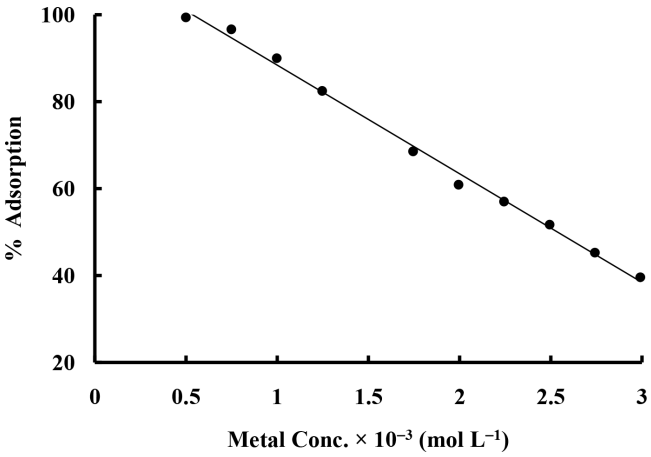

Fig. 9. Adsorption of mercury ions as a function of its own concentration on LPC.

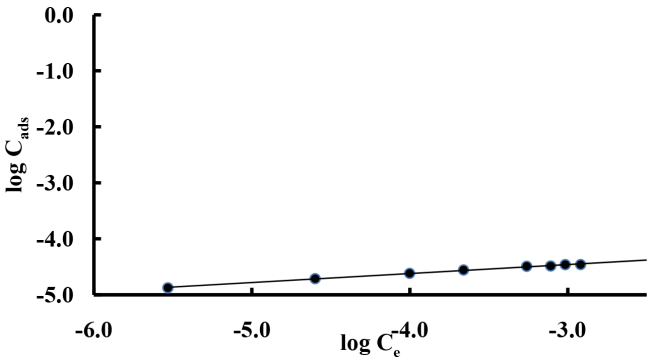

Fig. 10. Freundlich plot for the adsorption of mercury on LPC.

(21.10 mg g^{-1}) from Freundlich adsorption isotherm was compared with the reported values for different adsorbents and the results are shown in Table 2. The determined adsorption capacity in the present study is slightly lower than those of Fe_3O_4-graphene sheets and metal sulfide porous carbon complex but is higher than the reported values for magnetic mesoporous silica composites, multiwalled carbon nanotubes, polyhedral oligomeric silsesquioxane, clay, amine-modified attapulgite, black oak bark, chitosan coated magnetic nanoparticles, Ag/grapheme, Nitrogen-doped mesoporous carbon and Polypyrrole/SBA-15 nanocomposite.

3.5.1.2. Langmuir isotherm

According to the Langmuir adsorption isotherm all sites have equal affinity for the metal.

$$C_{ad} = \frac{QbC_e}{1 + bC_e} \tag{12}$$

The linear form of Langmuir adsorption isotherm may be written as

$$\frac{C_e}{C_{ad}} = \frac{1}{Qb} + \frac{C_e}{Q} \tag{13}$$

Table 2
Adsorption capacities of mercury for different adsorbents

Adsorbent	Capacity mg g^{-1}	References
Magnetic mesoporous silica composites	19.80	[54]
Fe_3O_4- graphene sheets	23.10	[55]
Multi-walled carbon nanotubes	13.16	[56]
Polyhedral oligomeric silsesquioxane	12.90	[57]
Clay	9.70	[58]
Amine-modified attapulgite	5.00	[59]
Black oak bark	4.00	[60]
Chitosan coated magnetic nanoparticles	10.00	[61]
Ag/graphene	5.40	[62]
Metal sulfide porouscarbon complex	23.00	[63]
Nitrogen-doped mesoporous carbon	13.89	[64]
Polypyrrole/SBA-15 nanocomposite	2.32	[65]
Low-rank Pakistani coal	21.10	Present work

where C_{ad} = concentration of mercury adsorbed at equilibrium (mol g^{-1}); C_e = equilibrium concentration of mercury in solution (mol L^{-1}); Q and b are Langmuir isotherm constants. A plot of C_e/C_{ad} against C_e gives a straight line (Fig. 11).

This linear plot supports the validity of the Langmuir model in the present work. The values of Langmuir constants Q and b calculated from the slope and intercept of the plot in Fig. 11 and were found to be 3.531 × 10^{-2} m mol g^{-1} and 28.522 × 10^3 dm^3 mol^{-1}, respectively.

The value of adsorption capacity (K_f) calculated from Freundlich isotherm is greater than Langmuir. Langmuir isotherm reflects only the mono-layer sorption of the LPC and therefore the adsorption capacity is lower than Freundlich sorption isotherm.

3.5.1.3. Dubinin-Radushkevich isotherm

The D-R isotherm was also applied in its linearized form to classify the chemical or physical adsorption.

$$C_{ad} = C_m \exp\left(-\beta \epsilon^2\right) \tag{14}$$

where C_{ad} is the amount of mercury sorbed on LPC, C_m is the maximum amount of mercury that can be sorbed on LPC using the optimized experimental conditions, ε is Polanyi potential and is a constant with a dimension of energy.

$$\varepsilon = RT \ln\left(1 + \frac{1}{C_e}\right) \tag{15}$$

where R = ideal gas constant; T = absolute temperature; C_e = equilibrium concentration of mercury in solution.

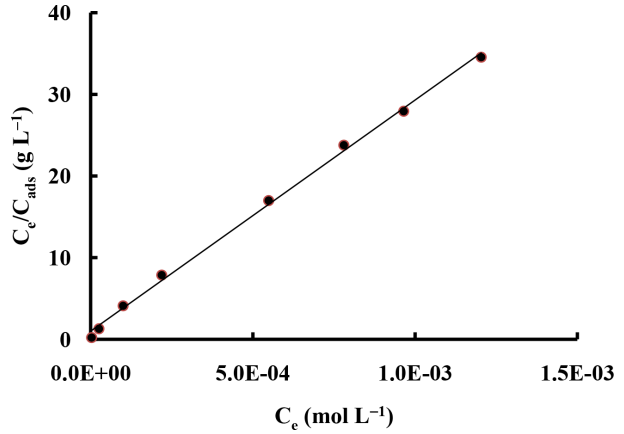

Fig. 11. Langmuir isotherm for the adsorption of mercury on LPC.

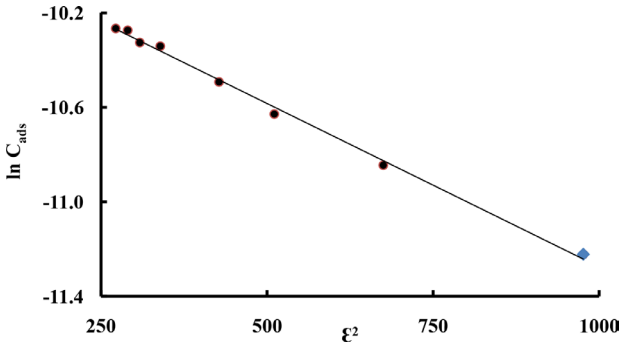

Fig. 12. D-R plot for the adsorption of mercury on LPC.

The linear form of D-R isotherm can be written as

$$\ln C_{ad} = \ln C_m - \beta\varepsilon^2 \tag{16}$$

A straight line was obtained when ln C_{ad} is plotted against ε^2 (Fig. 12) indicating that mercury ions adsorption also obeys the D-R equation. The determined adsorption capacity was found to be 5.057 × 10^{-2} m mol g^{-1}. The value of β was obtained from the linear D-R plot and was found to be 1.4 × 10^{-3} K J^2 mol^{-2}. By substituting the value of the mean sorption energy (E_s) was determined using Eq. (16) as:

$$E_S = \frac{1}{\sqrt{(-2\beta)}} \tag{17}$$

The values of adsorption free energy (E_s) for physical sorption is in the range of 1.0–8.0 kJ mol^{-1}, and greater than 8.0 kJ mol^{-1} for chemical sorption [66]. The determined value of E_s from Eq. (16) was 18.898 kJ mol^{-1}, indicated chemical sorption or ion exchange process.

The applicability of different non-linear models is generally judged by means of the Chi-square test (χ^2) values as determining tool for the best-fit adsorption isotherm equations which may be calculated by the following expression:

$$\chi^2 = \Sigma \frac{\left(C_{ads} - C_{ads,m}\right)^2}{C_{ads,m}} \tag{18}$$

where C_{ads}= equilibrium capacity from experimental data (mol g^{-1}); $C_{ads,m}$ = calculated equilibrium capacity from the model (mol g^{-1}).

To optimize the non-linear models one has to select certain equation parameters in such a way that a minimum value of Chi-square (χ^2) should be attained. In the present study, the Wave metrices software IGOR Pro 6.1.2, was used for the calculation of isotherm parameters of non-linear equations [Eqs. (10), (12) and (14)] for Freundlich, Langmuir and Dubinin-Radushkevich isotherm models, respectively. The non-linear plots of Langmuir, Freundlich and Dubinin-Radushkevich adsorption isotherms of mercury ions on coal were obtained by plotting C_e vs. C_{ads} (Fig. 13). The determined constants and theoretically calculated values are given in Table 3, which indicates that the determined values of adsorption capacities by the non-linear models are in quite comparable with those obtained by linear models.

3.6. Effect of temperature

The adsorption of 1.246×10^{-3} mol L^{-1} of mercury ions on LPC was carried out at different temperatures (283–333 K) using optimized parameters, and the results are shown in Table 4. It was found that the mercury ions adsorption increases with the increase in temperature.

Van't Hoff plot [67] was used to determine the values of ΔH and ΔS from the slope and intercept respectively, by using the following equation.

$$\ln K_c = \frac{\Delta S}{R} - \frac{\Delta H}{RT} \tag{19}$$

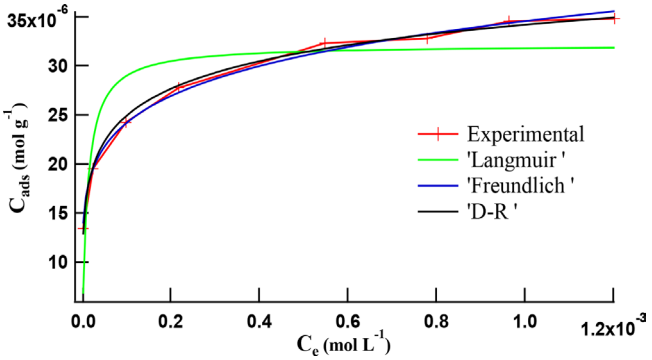

Fig. 13. Nonlinear plots of Langmuir, Freundlich and D-R isotherms for the adsorption of mercury on LPC.

where ΔH, K_c, R, ΔS and T are enthalpy change, equilibrium constant gas constant, change in entropy and absolute temperature for the adsorption process.

The equilibrium constant (K_c) was determined by using the relationship (20):

$$K_C = \frac{C_{eq.s}}{C_{eq.L}} \tag{20}$$

where $C_{eq.S}$ = equilibrium concentration of mercury adsorbed on the LPC (mg L^{-1}) and $C_{eq.L}$ = equilibrium concentration of mercury in solution (mg L^{-1}).

ΔG and ΔS for the specific sorption process have also been calculated using the relations:

$$\Delta G = -RT \ln K_c \tag{21}$$

$$\Delta S = \frac{\Delta H - \Delta G}{T} \tag{22}$$

ΔS and ΔH were calculated from the intercept and slope of the Van't Hoff plot, which is a plot of lnK_c against 1/T (Fig. 14), respectively.

The calculated values of ΔS, ΔG and ΔH have been presented in Table 5. The negative values of ΔG represent that the adsorption of mercury on LPC is a spontaneous process. The increase in the numerical value of −ΔG with the rise in temperature indicates that the adsorption process of mercury ions on LPC is more favorable at higher temperatures. The positive values of enthalpy (ΔH) change represent the endothermic nature of the sorption process. Since diffusion is an endothermic process, it was studied that increased solution temperature resulted in increased sorption of mercury ions. The positive value of entropy change (ΔS) indicates increase in the randomness of the system due to the adsorption of mercury ions on LPC.

3.7. Influence of diverse ions:

The presence of other cations and anions in the adsorptive phase may affect the environment and solution chemistry of the mercury ion, which influences the sorption efficiency of LPC. Therefore, using the optimized parameters, the sorption of 4.985×10^{-4} mol L^{-1} mercury ions on LPC was also studied in the presence of high concentrations of foreign ions. The anions were used as their sodium salts, while for cations the nitrate salts were used. The results are summarized in Table 6. The results show that adsorption efficiency of mercury on LPC was decreased

Table 3
Determined Freundlich, Langmuir & D-R isotherm parameters for Hg^{2+} ions adsorption on coal using non linear equations

Isotherm model	Parameters		± S.D	Chi square
Freundlich	n	6.426	0.221	2.058×10^{-12}
	K (m mol g^{-1})	0.101	4.28×10^{-6}	
Langmuir	Q (m mol g^{-1})	0.0321	1.91×10^{-6}	1.002×10^{-10}
	β	91033	4.64 × 104	
Dubinin-Radushkevich	C_m (m mol g^{-1})	0.0514	9.00×10^{-7}	1.528×10^{-12}
	β	6.2976×10^{-9}	1.92×10^{-10}	

Table 4
Adsorption behavior of mercury ions on LPC as a function of temperature

Dose of LPC			0.15 g		
Shaking time			10 min		
Volume equilibrated			4.0 cm^3		
pH			5.0		
Mercury ions concentration			1.246×10^{-3} mol L^{-1}		
Temp. (K)	1/T (K^{-1})	Concentration adsorbed (mol L^{-1})	Concentration in bulk (mol L^{-1})	K_c	ln K_c
283	3.534×10^{-3}	1.023×10^{-3}	2.227×10^{-4}	4.596	1.525
293	3.413×10^{-3}	1.073×10^{-3}	1.728×10^{-4}	6.211	1.826
298	3.356×10^{-3}	1.085×10^{-3}	1.611×10^{-4}	6.735	1.907
303	3.300×10^{-3}	1.122×10^{-3}	1.243×10^{-4}	9.027	2.200
313	3.195×10^{-3}	1.147×10^{-3}	9.892×10^{-5}	11.596	2.451
323	3.096×10^{-3}	1.173×10^{-3}	7.261×10^{-5}	16.161	2.783
333	3.003×10^{-3}	1.197×10^{-3}	4.892×10^{-5}	24.470	3.197

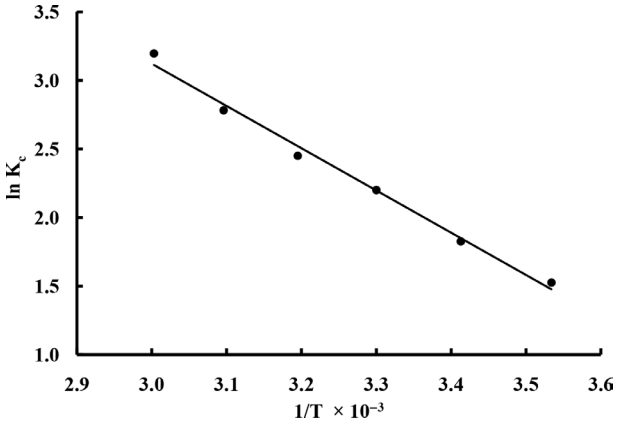

Fig. 14. Van't Hoff plot for the adsorption of mercury ions on LPC.

Table 5
Thermodynamic parameters for adsorption of mercury ions on LPC

Temperature (K)	ΔG (KJ mol^{-1})	ΔH (KJ mol^{-1})	ΔS (JK^{-1} mol^{-1})
283	–3.589	25.632	0.103
293	–4.449		0.103
298	–4.726		0.102
303	–5.543		0.103
313	–6.377		0.102
323	–7.472		0.102
333	–8.852		0.104

in the presence of bromide, nitrite and borate anions up to 61%. On the other hand adsorption of Hg(II) on LPC was decreased due to the presence of potassium, boron, germanium, iron, antimony, lead, zinc, cobalt, calcium, nickel and sodium cations up to 71%. This decrease in the sorption efficiency of mercury may be due to the competitor action of cations for the active sites present on the surface of LPC or the formation of stable complexes/compounds with anions.

3.8. Recycling process

To be useful in mercury ion recycling processes, adsorbed mercury ions should be easily desorbed under suitable conditions. Desorption experiments were carried out by using 1.0 M HNO_3 as the desorption agent. LPC adsorbed with the maximum concentration of mercury ions placed within the desorption medium, and shaken for 10 min. The desorbed mercury ions were determined by radio tracer technique. It was observed that 80% of mercury was desorbed in 10 min. This clearly shows that the LPC can be reused for the adsorption of mercury ions from aqueous solutions.

3.9. Applicability of the developed method

To check the applicability and efficiency for the removal of mercury ions from aqueous medium, the developed procedure was applied for the removal of mercury ions from a real tap water sample using the optimized conditions. Due to very low concentration of mercury in the sample it was spiked with 4.985×10^{-4} mol L^{-1} of mercury ions in 1.0×10^{-4} mol L^{-1} of nitric acid medium and shaked with 0.25 g of LPC for 10 min. The removal efficiency of mercury ion was found to be 95% in a single step, indicating that the developed procedure may be applied for the decontamination of mercury from such matrices. The determined composition of tap water sample is shown in Table 7.

4. Conclusions

The present study revealed that the LPC has good potential for the sorption of mercury from aqueous solutions. The sorption of mercury on LPC follows the pseudo-second

Table 6
Effect of diverse ions on the adsorption of 4.985×10^{-4} mol L^{-1} of mercury ions on LPC

Cation	Concentration (mol L^{-1})	Adsorption%	Anion	Concentration (mol L^{-1})	Adsorption %
No cation	–	99.70	No anion	–	99.70
Sodium	8.703×10^{-3}	92.12	Carbonate	3.333×10^{-3}	98.24
Potassium	5.128×10^{-3}	28.64	Bicarbonate	3.279×10^{-3}	98.31
Magnesium	8.230×10^{-3}	97.69	Nitrate	3.226×10^{-3}	99.81
Calcium	5.000×10^{-3}	71.80	Flouride	1.053×10^{-2}	99.31
Copper	3.147×10^{-3}	99.30	Nitrite	4.348×10^{-3}	53.67
Iron	3.582×10^{-3}	49.62	Phosphate	2.106×10^{-3}	97.94
Lead	9.653×10^{-4}	54.52	Bromide	2.503×10^{-3}	38.87
Cobalt	3.394×10^{-3}	68.06	Cyanide	7.692×10^{-3}	98.81
Aluminium	7.413×10^{-3}	96.82	Oxalate	2.273×10^{-3}	99.15
Boron	1.850×10^{-2}	30.91	Perchlorate	2.011×10^{-3}	98.87
Nickle	3.407×10^{-3}	89.31	Borate	3.401×10^{-3}	94.81
Antimony	1.643×10^{-3}	52.27	Chloride	5.641×10^{-3}	98.01
Zinc	3.059×10^{-3}	60.46	Iodide	1.576×10^{-3}	98.01
Cadmium	1.779×10^{-3}	100.00	Sulphide	6.238×10^{-3}	99.21
Germanium	2.755×10^{-3}	37.67	Citrate	3.390×10^{-3}	98.15

Table 7
Determined composition of tap water sample

Cations/anions	Concentration (mg L^{-1})
Ca^{+2}	30.42
Mg^{+2}	12.60
Na^{+}	18.42
K^{+}	3.23
Fe^{+3}	0.02
Mn^{+2}	0.01
Zn^{+2}	0.11
Cu^{+2}	0.01
Pb^{+2}	0.01
CO_3^{-2}	6.00
HCO_3^{-2}	108.00
Cl^{-}	3.80
NO_3^{-}	1.80
SO_4^{-2}	10.20
Hg^{+2}	100.00*
Hg^{+2}	5.01**

*Concentration after spiking

**Concentration after decontamination

order rate expression with intra particle diffusion process. The mercury adsorption data followed the Langmuir, Freundlich and Dubinin-Radushkevich isotherms. The sorption of mercury was increased with the rise in temperature. The thermodynamic parameters i.e. ΔG and ΔH represent spontaneity and endothermicity of mercury ion sorption on LPC. Sorption of mercury from tap water sample indicates that the proposed method is efficient and rapid in presence of various other ions. On the basis of this study it is concluded that the abundantly available, inexpensive, LPC has great potential for the adsorption of mercury ions from polluted environmental aqueous systems.

Acknowledgments

One of the authors i.e., Tariq Javed, would like to acknowledge the Higher Education Commission, Islamabad, Pakistan, for the award of an indigenous Ph. D. fellowship and Pakistan Institute of Nuclear Science and Technology, Islamabad, Pakistan, for providing research facilities for the present work.

References

[1] P.H. Kansenen, J. Venetvaara, Comparison of biological collectors of airborne heavy metals near ferrochrome and steel works, Water Air Soil Pollut., 60 (1991) 337–359.
[2] M. Gavrilescu, Removal of heavy metals from the environment by biosorption, Eng. Life. Sci., 4 (2004) 219–232.
[3] S.D. Pelo, E. Musu, R. Cidu, F. Frau, P. Lattanzi, Release of toxic elements from rocks and mine wastes at the Furtei gold mine (Sardinia, Italy), J. Geochem. Explor., 100 (2009) 142–152.
[4] J. Dong, Z. Xu, F. Wang, Engineering and characterization of mesoporous silica coated magnetic particles for mercury removal from industrial effluents, Appl. Surf. Sci., 254 (2008) 3522–3530.
[5] A.K. Meena, G.K. Mishra, P.K. Rai, C. Rajagopal, P.N. Nagar, Removal of heavy metal ions from aqueous solutions using carbon aerogel as an adsorbent, J. Hazard. Mater., 122 (2005) 161–170.
[6] X.L.J. Xie, J. Liang, Absorbency and adsorption of poly (acrylic acidco-acrylamide) hydrogel, J. Appl. Polym. Sci., 106 (2007) 1606–1613.
[7] L.C. Chasar, B.C. Scudder, A.R. Stewart, A.H. Bell, G.R. Aiken, Mercury cycling in stream ecosystems, trophic dynamics and methyl mercury bioaccumulation, Environ. Sci. Technol., 43 (2009) 2733–2739.

[8] S.W. Tan, J.C. Meiller, K.R. Mahaffey, The endocrine effects of mercury in humans and wildlife, Crit. Rev. Toxicol., 39 (2009) 228–269.
[9] X. Zhu, Y. Kusaka, K. Sato, Q. Zhang, The endocrine disruptive effects of mercury, Environ. Health Prev. Med., 4 (2000) 174–183.
[10] O.S. Amuda, I.A. Amoo, O.O. Ajayi, Performance optimization of coagulant/flocculant in the treatment of wastewater from a beverage industry, J. Hazard. Mater., 129 (2006) 69–72.
[11] Y.K. Henneberry, T.E.C. Kraus, J.A. Fleck, D.P. Krabbenhoft, P.M. Bachand, W.R. Horwath, Removal of inorganic mercury and methyl mercury from surface waters following coagulation of dissolved organic matter with metal-based salts, Sci. Total Environ., 409 (2011) 631–637.
[12] Y. Ku, M.H. Wu, Y.S. Shen, Mercury removal from aqueous solutions by zinc cementation, Waste Manage., 22 (2002) 721–726.
[13] Z. Li, Q. Wei, R. Yuan, X. Zhou, H. Liu, H. Shan, Q. Song, A new room temperature ionic liquid 1-butyl-3-trimethylsilylimidazolium hexafluorophosphate as a solvent for extraction and preconcentration of mercury with determination by cold vapor atomic absorption spectrometry, Talanta, 71 (2007) 68–72.
[14] M.L.P. Reddy, T. Francis, Recent advances in the solvent extraction of mercury (II) with calixarenes and crown ethers, Solvent Extr. Ion Exc., 19 (2001) 839–863.
[15] D.S. Han, M. Orillano, A. Khodary, Y. Duan, B. Batchelor, A. Abdel-Wahaba, Reactive iron sulfide (FeS)-supported ultra filtration for removal of mercury (Hg(II)) from water, Water Res., 53 (2014) 310–321.
[16] Y. Huang, J.R. Du, Y. Zhang, D. Lawless, X. Feng, Removal of mercury (II) from wastewater by polyvinylamine-enhanced ultra filtration, Sep. Purif. Technol., 154 (2015) 1–10.
[17] T.S. Anirudhan, L. Divya, M. Ramachandran, Mercury(II) removal from aqueous solutions and waste waters using a novel cation exchanger derived from coconut coir pith and its recovery, J. Hazard. Mater., 157 (2008) 620–627.
[18] A. Oehmen, D. Vergel, J. Fradinho, M.A.M. Reis, J.G. Crespo, S. Velizarov Mercury removal from water streams through the ion exchange membrane bioreactor concept, J. Hazard. Mater., 264 (2014) 65–70.
[19] J.B. Zambrano, S. Laborie, P. Viers, M. Rakib, G. Durand, Mercury removal and recovery from aqueous solutions by coupled complexation-ultra filtration and electrolysis, J. Membr. Sci., 229 (2004) 179–186.
[20] C. Aydiner, M. Bayramoglu, S. Kara, B. Keskinler, O. Ince, nickel removal from water using surfactant-enhanced hybrid PAC/MF process, the influence of system-component variables, Ind. Eng. Chem. Res., 45 (2006) 3926–3933.
[21] M.M. Matlock, B.S. Howerton, D.A. Atwood, Irreversible precipitation of mercury and lead, J. Hazard. Mater., 84 (2001) 73–82.
[22] L.Y. Blue, P. Jana, D.A. Atwood, Aqueous mercury precipitation with the synthetic dithiolate, BDTH2, Fuel, 89(6) (2010) 1326–1330.
[23] S. Manchester, X. Wang, I. Kulaots, Y. Gao, R.H. Hurt, High capacity mercury adsorption on freshly ozone-treated carbon surfaces, Carbon, 46 (2008) 518–524.
[24] S. Wang, H. Wu, Environmental-benign utilisation of fly ash as low-cost adsorbents, J. Hazard. Mater., 136 (2006) 482–501.
[25] N. Asasian, T. Kaghazchi, Sulfurized activated carbons and their mercury adsorption/desorption behavior in aqueous phase, Int. J. Environ. Sci. Technol., 12(8) (2015) 2511–2522.
[26] X.W. Wu, H.W. Ma, J.H. Li, J. Zhang, Z.H. Li, The synthesis of mesoporous aluminosilicate using microcline for adsorption of mercury(II), J. Colloid Interface Sci., 315 (2007) 555–561.
[27] C.B. Lopes, M. Otero, Z. Lin, C.M. Silva, J. Rocha, E. Pereira, A.C. Duarte, Removal of Hg^{2+} ions from aqueous solution by ETS-4 micro porous titanosilicate kinetic and equilibrium studies, Chem. Eng. J., 151 (2009) 247–254.
[28] L.A. Belyakova, O.M. Shvets, D.Y. Lyashenko, Formation of the nanostructure on a silica surface as mercury(II) ions adsorption sites, Inorg. Chim. Acta, 362 (2009) 2222–2230.
[29] Q.Z. Zhai, Nano α-Al_2O_3 for removal of Hg(II) from water: Adsorption and desorption studies, J. Chem. Pharm. Res., 6(5) (2014) 1310–1317.
[30] J. Aguado, J.M. Arsuaga, A. Arencibia, Influence of synthesis conditions on mercury adsorption capacity of propylthiol functionalized SBA-15 obtained by co-condensation, Micro porous Meso porous Mater., 109 (2008) 513–524.
[31] J. Goel, K. Kadirvelu, C. Rajagopal, V.K. Garg, Removal of mercury(II) from aqueous solution by adsorption on carbon aerogel: response surface methodological approach, Carbon, 43 (2005) 197–200.
[32] M.A. Lopez-Anton, P. Abad-Valle, M. Diaz-Somoano, I. Suarez-Ruiz M.R. Martinez-Tarazona, The influence of carbon particle type in fly ashes on mercury adsorption, Fuel, 88 (2009) 1194–1200.
[33] S.T. Chung, K.I. Kim, Y.R. Yun, Adsorption of elemental mercury vapor by impregnated activated carbon from a commercial respirator cartridge, Powder Technol., 192 (2009) 47–53.
[34] D.L. Guerra, R.R. Viana, C. Airoldi, Adsorption of mercury cation on chemically modified clay, Mater. Res. Bull., 44 (2009) 485–491.
[35] M.S. Shaukat, M.I. Sarwar, R. Qadeer, Adsorption of strontium ions from aqueous solution on Pakistani coal, J. Radioanal. Nucl. Chem., 265 (2005) 73–79.
[36] J. Anwar, U. Shafique, M. Salman, W. Zaman, S. Anwar, J.M. Anzano, Removal of chromium (III) by using coal as adsorbent, J. Hazard. Mater., 171 (2009) 797–801.
[37] T. Javed, N. Khalid, M.L. Mirza, Adsorption characteristics of copper ions on low-rank Pakistani coal, Desal. Water Treat., 59 (2017) 181–190.
[38] T. Javed, N. Khalid, M.L. Mirza, Removal of lead ions from aqueous solutions by low-rank Pakistani coal, Desal. Water Treat., 81 (2017) 133–142.
[39] A. Periasamy, S. Murugan, M. Palaniswamy, Vibrational studies of Na_2SO_4, K_2SO_4, $NaHSO_4$ and $KHSO_4$ crystals, Rasayan J. Chem., 2(4) (2009) 981–989.
[40] S. Yao, K. Zhang, K. Jiao, W. Hu, Evolution of coal structures: FTIR analyses of experimental simulations and naturally matured coals in the Ordos Basin, China, Energ. Explor. Exploit., 29(1) (2011) 1–19.
[41] M. Shafiabadi, A. Dashti, H. Tayebi, Removal of Hg (II) from aqueous solution using polypyrrole/SBA-15 nanocomposite: Experimental and modeling, Synthetic Met., 212 (2016) 154–160.
[42] D.L. Pavia, G.M. Lampman, G.S. Kriz, J.R. Vyvyan, Introduction to spectroscopy, 5th Edition, Cengage Learning, Andover, (2015).
[43] S.K. Kazy, S.F. D'Souza, P. Sar, Uranium and thorium sequestration by a Pseudomonas sp.: Mechanism and chemical characterization, J. Hazard. Mater., 163 (2009) 65–72.
[44] V.C. Srivastava, I.D. Mall, I.M. Mishra, Characterization of mesoporous rice husk ash (RHA) and adsorption kinetics of metal ions from aqueous solution onto RHA, J. Hazard. Mater., B134 (2006) 257–267.
[45] L. Norton, K. Baskaran, T. McKenzie, Biosorption of zinc from aqueous solution using biosolids, Adv. Environ. Res., 8 (2004) 629–635.
[46] V. Vimonses, B. Jin, C.W.K Chow, C. Saint, An adsorption photo catalysis hybrid system as alternative wastewater treatment by multi-functional nanoporous materials, Water Res., 44 (2010) 5385–5397.
[47] C. Arpa, E. Basyilmaz, S. Bektas, O. Genc, Y. Yurum, Cation exchange properties of low rank Turkish coals: removal of Hg, Cd and Pb from waste water, Fuel Process. Technol., 68(2) (2000) 111–120.
[48] S. Karabulut, A. Karabakan, A. Denizli, Y. Yurum, Cadmium (II) and mercury (II) removal from aquatic solutions with low-rank Turkish coal, Sep. Sci. Technol., 36(16) (2001) 3657–3671.
[49] C. Lao, Z. Zeledon, X. Gamisans, M. Sole, Sorption of Cd(II) and Pb(II) from aqueous solutions by a low-rank coal (leonardite), Sep. Purif. Technol., 45 (2005) 79–85.

[50] W.J. Weber, J.C. Morris, Kinetics of adsorption on carbon from solution, J. Sanit. Eng. Div., Am. Soc. Civ. Eng., 89 (1963) 31–59.
[51] T. Javed, N. Khalid, M.L. Mirza, Kinetics, isotherm and thermodynamics for thorium ions adsorption from aqueous solutions by coal, Desal. Water Treat., 92 (2017) 291–300.
[52] D. Reichenberg, Properties of ion exchange resins in relation to their structure. III. Kinetics of exchange, J. Am. Chem. Soc., 75 (1953) 589–597.
[53] S. Zafar, N. Khalid, M.L. Mirza, Potential of rice husk for the decontamination of silver ions from aqueous media, Sep. Sci. Technol., 47 (2012) 1793–1801.
[54] C.F. Carolin, P.S. Kumar, A. Saravanan, G.J. Joshiba, M. Naushad, Efficient techniques for the removal of toxic heavy metals from aquatic environment: a review, J. Environ. Chem. Eng., 5 (2017) 2782–2799.
[55] M. Ghasemi, M. Naushad, N. Ghasemi, Y. Khosravi-fard, A novel agricultural waste based adsorbent for the removal of Pb(II) from aqueous solution: kinetics, equilibrium and thermodynamic studies, J. Ind. Eng. Chem., 20 (2014) 454–461.
[56] B. Tawabini, S.A. Khaldi, M. Atieh, M. Khaled, Removal of mercury from water by multi-walled carbon nanotubes, Water Sci. Technol., 61 (2010) 591–598.
[57] W.J. Wang, M.L. Chen, X.W. Chen, J.H. Wang, Thiol-rich polyhedral oligomeric silsesquioxane as a novel adsorbent for mercury adsorption and speciation, Chem. Eng. J., 242 (2014) 62–68.
[58] M. Eloussaief, A. Sdiri, M. Benzina, Modelling the adsorption of mercury onto natural and aluminium pillared clays, Environ. Sci. Pollut. Res., 20 (2013) 469–479.
[59] H. Cui, Y. Qian, Q. Li, Z.B. Wei, J.P. Zhai, Fast removal of Hg(II) ions from aqueous solution by amine-modified attapulgite, Appl. Clay. Sci., 72 (2013) 84–90.
[60] L.A. Teles de Vasconcelos, C.G. Gonzalez Beca, Adsorption equilibria between pine bark and several ions in aqueous solution, Eur. Water Pollut. Control, 4(1) (1994) 41–51.
[61] S. Nasirimoghaddam, S. Zeinali, S. Sabbaghi, Chitosan coated magnetic nanoparticles as nano-adsorbent for efficient removal of mercury contents from industrial aqueous and oily samples, J. Ind. Eng. Chem., 27 (2015) 79–87.
[62] Z. Qu, L. Fang, D. Chen, H. Xu, N. Yan, Effective and regenerable Ag/graphene adsorbent for Hg(II) removal from aqueous solution, Fuel, 203 (2017) 128–134.
[63] K.S.K. Reddy, A. Al Shoaibi, C. Srinivasakannan, Mercury removal using metal sulfide porous carbon complex, Process Saf. Environ., 114 (2018) 153–158.
[64] M. Naushad, T. Ahamad, M. Basheer. A. Maswari, A.A. Alqadami, S.M. Saad, Nickel ferrite bearing nitrogen-doped mesoporous carbon as efficient adsorbent for the removal of highly toxic metal ion from aqueous medium, Chem. Eng. J., 330 (2017) 1351–1360.
[65] M. Shafiabadi, A. Dashti, H. Tayebi, Removal of Hg (II) from aqueous solution using polypyrrole/SBA-15 nanocomposite: Experimental and modeling, Synthetic Met., 212 (2016) 154–160.
[66] M.M. Dubinin, L.V. Radushkevich, The equation of the characteristic curve of activated charcoal, Proc. Acad. Sci. USSR, Phy. Chem. Sec., 55 (1947) 331–337.
[67] T. Javed, N. Khalid, M.L. Mirza, Kinetics, equilibrium and thermodynamics of cerium removal by adsorption on low-rank coal, Desal. Water Treat., 89 (2017) 240–249.